Journal of Ceramic Processing Research. Vol. 18, No. 6, pp. 431~434 (2017)

J O U R N A L O F
Ceramic Processing Research

The ferroelectric properties of Ce-doped PZT/BFO multilayer thin films prepared using the sol-gel method

Mi-Ri Park, Sung-Gap Lee* Kyeong-Min Kim and Min-Su Kwon
Dept. of Materials Engineering and Convergence Technology, RIGET, Gyeongsang National University, Jinju 52828, Korea

In this study, Ce-doped PZT/BFO multilayer thin films were prepared by the spin-coating method on Pt(200 nm)/Ti(10 nm)/SiO_2(100 nm)/P-Si(100) substrates using $Bi_{0.9}Ce_{0.1}FeO_3$ and $Pb(Zr_{0.52}Ti_{0.48})O_3$ metal alkoxide solutions. The coating and heating procedure was repeated several times to form multilayer thin films. All PZT/BCFO multilayer thin films display the typical XRD pattern of a polycrystalline perovskite structure with a uniform, void-free grain microstructure. The thickness of the PZT and BCFO film after one cycle of drying/sintering was approximately 30 nm, and all films consist of fine grains with a relatively flat surface morphology. The relative dielectric constant and dielectric losses of the six-coated PZT/BCFO thin film were approximately 360 and 0.003%, respectively. As the number of coatings increased, the remanent polarization and coercive field increased. The values for the six-coated PZT/BCFO thin film were 17.6 μC/cm^2 and 53 kV/cm, respectively.

Key words: Bismuth ferrite, PZT, Multilayer film, Sol-gel method, Hysteresis loop.

Introduction

Multiferroic materials, which simultaneously exhibit ferroelectric and ferromagnetic (or antiferromagnetic) properties, provide opportunities for potential application in information storage, spintronic devices, and sensors [1-3]. Bismuth ferrite ($BiFeO_3$, BFO) is one such multiferroic material. BFO exhibits a distorted perovskite structure with a rhombohedral symmetry in the R3c space group, with a unit cell parameter a = 0.5643 nm and α = 59.348 º. BFO has a higher transition temperature than most multiferroic materials, that is, a Curie temperature of 850 ºC and a Neel temperature of 370 ºC [4, 5].

However, BFO has a serious leakage problem as a result of charge defects and second phases, which makes it difficult to achieve a well-saturated ferroelectric hysteresis loop and low dielectric loss, thus hindering its practical application. As a result, dielectric breakdown occurs easily even at a low field, thereby indicating the difficulty in poling a film. To overcome this problem, various approaches have been proposed, including a substitution technique using Mn and Ti at the B-site, La and/or Nd at the A-site, and the formation of a solid solution using $Pb(Zr,Ti)O_3$ and $BaTiO_3$ [6-10].

Singh et al. [11] reported that the leakage current and remanent polarization of BFO films reduced with an increase in La-doping concentration. The ionic radius of Ce(0.101 nm) is slightly smaller than that of La(0.103 nm) and Bi(0.103 nm). Therefore, it is expected that Ce-doping could reduce leakage current and induce structure distortions, improving the electrical properties of BFO films.

We have already reported on the good dielectric properties, especially the high remanent polarization and low leakage current densities of PZT hetero-layered thin films [12]. In this study, PZT/BCFO multilayer thin films were prepared using the sol-gel method, which were spin-coated on a Pt/Ti/SiO_2/Si substrate alternately using PZT and BCFO metal alkoxide solutions. We also investigated the structural and dielectric properties of PZT/BCFO multilayer thin films.

Experimental

$Bi_{0.9}Ce_{0.1}FeO_3$(BCFO) and $Pb(Zr_{0.52}Ti_{0.48})O_3$(PZT) with excess Pb-acetate 10 mol% precursor solutions were prepared by the sol-gel method from Bi-nitrate pentahydrate [$Bi(NO_3)_3 \cdot 5H_2O$], Ce-nitrate hexahydrate [$Ce(NO_3) \cdot 6H_2O$], Fe-nitrate nonahydrate [$Fe(NO_3)_3 \cdot 9H_2O$]. Pb-acetate trihydrate [$Pb(CH_3CO_2)_2 \cdot 3H_2O$], Zr n-propoxide [$Zr(OCH_2CH_2CH_3)_4$], and Ti iso-propoxide [$Ti[OCH(CH_3)_2]_4$] as starting materials, with 2-methoxyethanol as a solvent. The PZT precursor solution was passed through a syringe filter and spin-coated onto Pt(200nm)/Ti(10nm)/SiO2(100nm)/p-Si(100) substrates using a spinner operating at 3,000rpm for 25 seconds to form the first layer. These PZT films were dried at 350 ºC for 15 minutes to remove the organic materials, and sintered at 600 ºC for 30 minutes to crystallize them into a perovskite structure. A BCFO precursor solution was then spin-coated and dried on the PZT films under the same conditions, and sintered at 550 ºC

*Corresponding author:
Tel : +82-55-772-1687
Fax: +82-55-772-1689
E-mail: lsgap@gnu.ac.kr

for 10 minutes to form the second BCFO layer. This procedure was repeated several times to fabricate PZT/BCFO multilayer thin films. The crystalline structure of the PZT/BCFO multilayer films was analyzed by X-ray diffraction (XRD), and the surface and cross-sectional morphologies of the films were examined by scanning electron microscopy (SEM). To measure the ferroelectric properties, Pt films were DC sputter-deposited onto the PZT/BCFO films as the top electrode with a diameter of 500 μm. The leakage current and polarization electric field [P-E] hysteresis loops were analyzed using a ferroelectric test system (RT66B; Radiant Technologies, Inc., Albuquerque, NM, USA).

Results and Discussion

Fig. 1 shows the XRD patterns of PZT/BCFO multilayer thin films. All films displayed the typical XRD patterns of a perovskite polycrystalline structure, and a second phase such as $Bi_2Fe_4O_3$ or the preferred orientation was not observed. Generally, XRD patterns

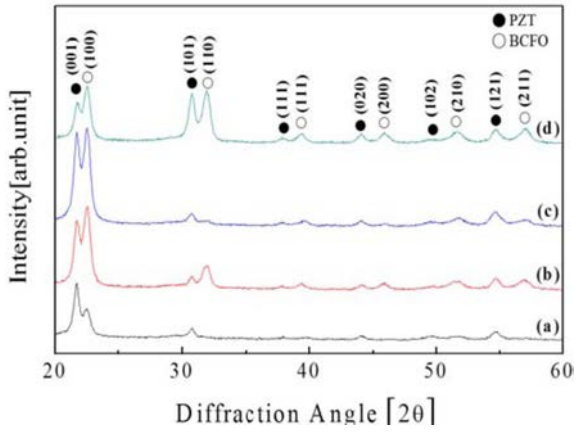

Fig. 1. XRD patterns of PZT/BCFO multilayer thin films : (a) 3-layers, (b) 4-layers, (c) 5-layers, (d) 6-layers.

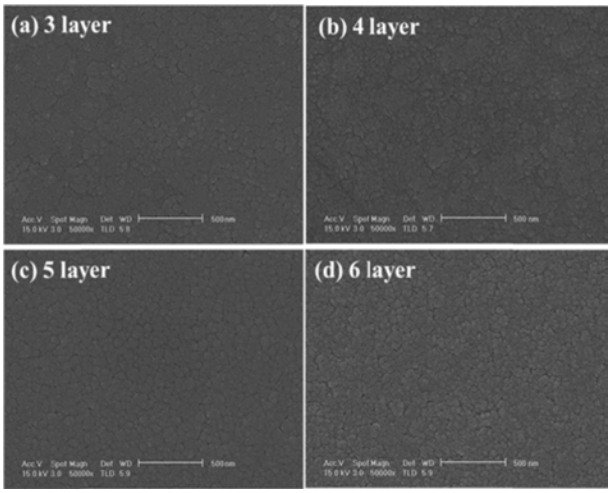

Fig. 2. FE-SEM surface images of PZT/BCFO multilayer thin films; (a) 3-layers, (b) 4-layers, (c) 5-layers, (d) 6-layers.

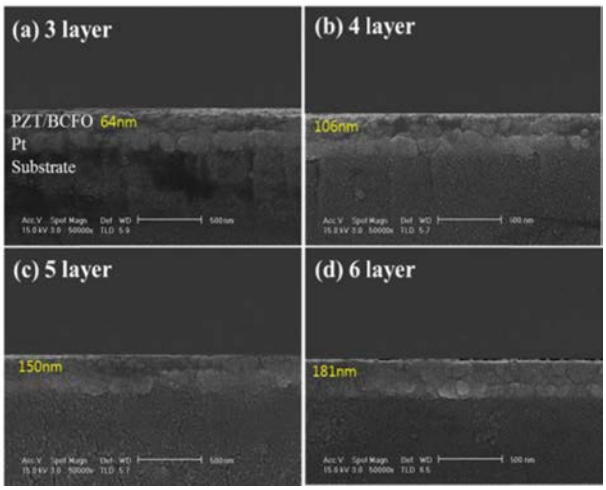

Fig. 3. FE-SEM cross-sectional images of PZT/BCFO multilayer thin films; (a) 3-layers, (b) 4-layers, (c) 5-layers, (d) 6-layers.

of PZT(52/48) thin films show a single peak for each diffraction angle. In addition, XRD patterns of BCFO films show a single peak at $2\theta = 22.5^{\circ}$ and 46°. However, all PZT/BCFO multilayer thin films showed that the XRD peak splits at each diffraction angle. This property can be attributed to the effect of the lower layer. Moreover, it can be assumed that the crystal growth of the upper BCFO (or PZT) layer can be influenced by the lower PZT (or BCFO) layer, and that the crystallization behavior of the resulting film is controlled by the choice of the initial or seed layer.

Figs. 2 and 3 show the surface and cross-sectional FE-SEM micrographs of PZT/BCFO multilayer thin films. The average thickness of the film after one cycle of drying/sintering was approximately 30-45 nm, and the thickness of the PZT/BCFO-6 film was 181 nm. All films consist of a fine grain structure with a relatively flat surface morphology. It is assumed that the lower BCFO (or PZT) layers play an important role as a nucleation site or seed layer for the formation of homogeneous and uniform upper PZT (or BCFO) layers.

Figs. 4 and 5 show the relative dielectric constant and dielectric losses of PZT/BCFO multilayer thin films as a function of the measuring frequency (from 1kHz to 1MHz). The relative dielectric constant decreased with an increase in the applied frequency, and the PZT/BCFO multilayer thin films exhibited typical frequency dispersion behavior. The dielectric constant increased and dielectric loss decreased with an increase in the number of coatings, and the PZT/BCFO-6 film at 1kHz displays good results of 360 and 0.003%, respectively. PZT/BCFO multilayer thin films exhibit a superior dielectric constant than a single-composition BFO film (166 at 1 kHz). This phenomenon can probably be attributed to the diffusion of Pb from the PZT film into the Pt bottom electrode, and the diffusion of Pb, Ti, Zr, Bi, Ce and Fe at the interfaces between the PZT film and the

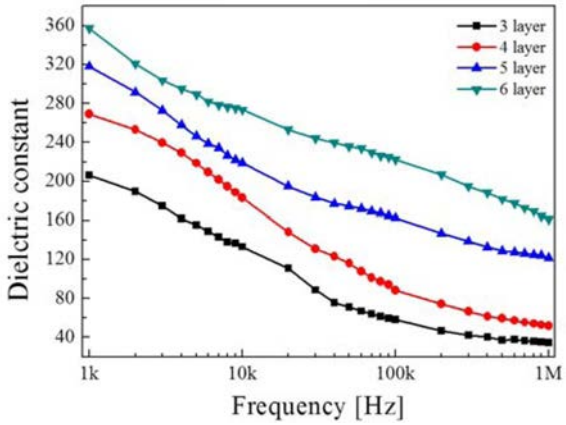

Fig. 5. The dielectric loss of the PZT/BCFO thin films ; (a) 3-layers, (b) 4-layers, (c) 5-layers, (d) 6-layers.

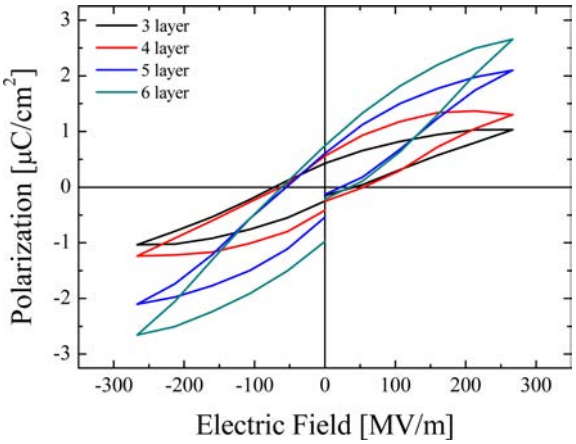

Fig. 6. P-E hysteresis loops of the PZT/BCFO thin films; (a) 3-layers, (b) 4-layers, (c) 5-layers, (d) 6-layers.

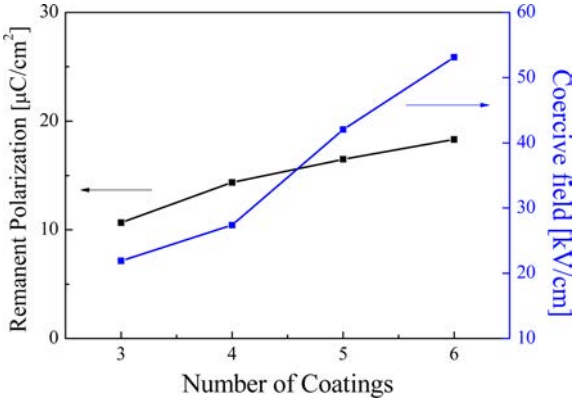

Fig. 7. Remanant polarization and coercive field of the PZT/BCFO thin films; (a) 3-layers, (b) 4-layers, (c) 5-layers, (d) 6-layers.

BCFO film is intensified with an increase in the number of layers, or in other words, an increase in the number of annealing processes [9]. Dielectric losses decreased with an increase in the number of layers because the interfaces between PZT and BCFO layers act as sinks for the charges. However, further investigation and discussion are necessary in order to fully understand the dielectric properties of PZT/BCFO multilayer films.

Fig. 6 shows the hysteresis loops of PZT/BCFO multilayer thin films. The centers of the hysteresis loops are not located at zero bias voltage, but are shifted toward negative bias voltage. It is suggested that an internal bias field has been induced at the interface between the lower electrode and the PZT films due to the difference in thermal history between the upper and lower electrodes.

Fig. 7 shows the variation in the remanent polarization and coercive field of the PZT/BCFO thin films based on the number of layers. The remanent polarization and coercive field may be attributed to an increase in the formation of second phases with low permittivity at the interfaces between layers as well as sinks that trap charges forming at interfaces. These second phases act as sinks for charges and inhibit their spatial movement. As a result, the coercive field increased with a increase in the number of layers. The remanent polarization and coercive field of the PZT/BCFO-6layers were 17.6 μC/cm^2 and 53 kV/cm, respectively.

Conclusions

In this study, $Pb(Zr_{0.52}Ti_{0.48})O_3$ and $BiCeFeO_3$ alkoxide solutions were prepared by the sol-gel method, and PZT/BCFO multilayer thin films were spin-coated onto a Pt/Ti/SiO_2/Si substrate alternately using PZT(52/48) and BCFO alkoxide solutions. The thickness of the PZT and BCFO film after one cycle of drying/sintering was approximately 30nm, and all films consist of fine grains with a relatively flat surface morphology. The reason for this is assumed to be that the lower layers play an important role as a nucleation site or seed layer for the formation of homogeneous and uniform upper layers. Dielectric properties such as dielectric constant, dielectric loss, and remanent polarization of PZT/BCFO multilayer thin films were superior to those of single-composition BFO films, and the values for the PZT/BCFO-6 film were 360, 0.003%, and 17.6μC/cm^2, respectively. We believe that these properties of PZT/BCFO multilayer films were caused by interface effects between the PZT and BCFO films.

References

1. M. Fiebig, T. Lottermoser, D. Meier and M. Trassin, Nature Reviews Materials 1 (2016) 16046.
2. L.W. Martin, Dalton Transactions 39 (2010) 10813-10826.
3. W. Eerenstein, N.D. Mathur, J.F. Scott, Nature 442 (2006) 759-765.
4. H. Liu, Y. Sun and X. Wang, J. phys. D: Appl. Phys. 41 (2008) 095302.
5. S. Yakovlev, J. Zekonyte, C.-H. Solterbeck, M. Es-Souni, Thin Solid Films 493 (2005) 24-29.
6. L. Chen, W. Ren, W. Zhu, Z.-G. Ye, P. Shi, X. Chen, Thin Solid Films 518 (2010) 1637-1640.

7. J.H. Kim, H. Funakubo, Y. Sugiyama, and H. Ishiwara, Jpn. J. Appl. Phys. 48 (2009) 09KB02.
8. Y. Hamazaki, W. Sakamoto, M. Moriya, and T. Yogo, Jpn. J. Appl. Phys. 48 (2009) 09KA08.
9. T. Kawae, Y. Terauchi, H. Tsuda, M. Kumeda, A. Morimoto, Appl. Phys. Lett. 94 (2009) 112904.
10. T. Ozaki, S. Mori, Jpn. J. Appl. Phys. 4 (2009) 09KC07.
11. S.K. Singh, H. Ishiwara, K. Sato, K. Maruyama, J. Appl. Phys. 102 (2007) 094109.
12. S.H. Jo, S.G. Lee and Y.H. Lee, Nanoscale Res. Lett. 7 (2012) 54-58.